The EMBO Journal Vol.16 No.8 pp.1992–2003, 1997

The activation domain of the MotA transcription factor from bacteriophage T4

Michael S.Finnin[1], Marco P.Cicero, Christopher Davies[2], Stephanie J.Porter[2], Stephen W.White[2,3] and Kenneth N.Kreuzer[3]

Department of Microbiology, Box 3020, Duke University Medical Center, Durham, NC 27710, USA

[1]Present address: Cellular Biochemistry and Biophysics Program, Memorial Sloan-Kettering Cancer Center, 1275 York Avenue, New York, NY 10021, USA
[2]Present address: Department of Structural Biology, St Jude Children's Research Hospital, 332 North Lauderdale Street, Memphis, TN 38105-2794, USA

[3]Corresponding authors
e-mail: kreuzer@abacus.mc.duke.edu and stephenwhite@stjude.org

Bacteriophage T4 encodes a transcription factor, MotA, that binds to the –30 region of middle-mode promoters and activates transcription by host RNA polymerase. We have solved the structure of the MotA activation domain to 2.2 Å by X-ray crystallography, and have also determined its secondary structure by NMR. An area on the surface of the protein has a distinctive patch that is populated with acidic and hydrophobic residues. Mutations within this patch cause a defective T4 growth phenotype, arguing that the patch is important for MotA function. One of the mutant MotA activation domains was purified and analyzed by NMR, and the spectra clearly show that the domain is properly folded. The mutant full-length protein appears to bind DNA normally but is deficient in transcriptional activation. We conclude that the acidic/hydrophobic surface patch is specifically involved in transcriptional activation, which is reminiscent of eukaryotic acidic activation domains.

Keywords: activation domain/nuclear magnetic resonance/site-directed mutagenesis/transcription factor/X-ray crystallography

Introduction

Although much has been learned about how transcription factors recognize their DNA target sites (Pabo and Sauer, 1992), relatively little is known about how these factors interact with the basal transcription apparatus to activate transcription. In prokaryotes, activation is generally achieved by a single activator protein that interacts with the α or σ-subunits of RNA polymerase (Ishihama, 1993; Busby and Ebright, 1994). In contrast, activation of eukaryotic transcription often involves multiple proteins, including activators that bind to DNA targets and co-activators necessary for communication between activators and the basal transcription apparatus (Smale, 1994; Zawel and Reinberg, 1995). The transcriptional activation and DNA-binding functions of eukaryotic activators are usually within separate protein domains, and several types of activation domains have been characterized (Ptashne and Gann, 1990).

We are studying the MotA transcriptional activator from bacteriophage T4. Bacteriophage T4 genes are transcribed by the host RNA polymerase from three classes of promoter in a temporal cascade. Early promoters resemble strong host promoters and are transcribed by unmodified RNA polymerase (Wilkens and Rüger, 1994). Middle-mode promoters have a standard –10 sequence (5′-TAN-NNT-3′), along with a unique consensus sequence [5′-(A/T)(A/T)TGCTT(T/C)-3′] in the –30 region (Brody *et al.*, 1983; Guild *et al.*, 1988; Stitt and Hinton, 1994). Activation of middle-mode promoters requires MotA, which binds the –30 consensus sequence (the mot box) and AsiA, which binds tightly to the host σ^{70}-subunit (deFranciscis *et al.*, 1982; Hinton, 1991; Schmidt and Kreuzer, 1992; Orsini *et al.*, 1993; Ouhammouch *et al.*, 1995). Finally, T4 late promoters require a phage-encoded σ-subunit and an enhancement mechanism that depends on T4 replication proteins (Williams *et al.*, 1994).

The existence of a T4 middle-mode transcription factor was first inferred from *in vitro* transcription/translation experiments using T4 DNA and an extract from uninfected *Escherichia coli* (O'Farrell and Gold, 1973). Subsequent genetic studies led to a collection of pleiotropic mutations that all mapped to the same gene, designated *motA* (for modifier of transcription; earlier designation, *mot*) (reviewed by Stitt and Hinton, 1994). Although these *motA* point mutations do not block phage growth in normal *E.coli* strains, the *motA* gene is essential because a *motA* deletion mutant phage cannot grow unless the MotA protein is supplied *in trans* (Benson and Kreuzer, 1992).

Detailed analyses of the MotA protein were greatly facilitated by the elucidation of the gene sequence (Uzan *et al.*, 1990) and the overproduction and purification of the protein (Hinton, 1991; Schmidt and Kreuzer, 1992). MotA has two ~10 kDa domains that can readily be separated by cleavage with trypsin, and NMR experiments have confirmed that each domain folds independently (Finnin *et al.*, 1993). The C-terminal domain (MotCF) binds DNA, and the N-terminal domain (MotNF) contains the activation elements (Finnin *et al.*, 1993, 1994; D.Hinton, personal communication; this report). The full-length MotA protein failed to crystallize and was too large for NMR analysis, and our structural studies have therefore employed cloned versions of the two MotA domains.

We previously determined the secondary structure of MotCF using NMR spectroscopy (Finnin *et al.*, 1994), and this domain resembles one-half of the eukaryotic TATA-binding protein (TBP) which is an intramolecular dimer (Nikolov *et al.*, 1992). In this communication, we report the analysis of the structure of the MotNF domain using both X-ray crystallography and NMR. The molecule

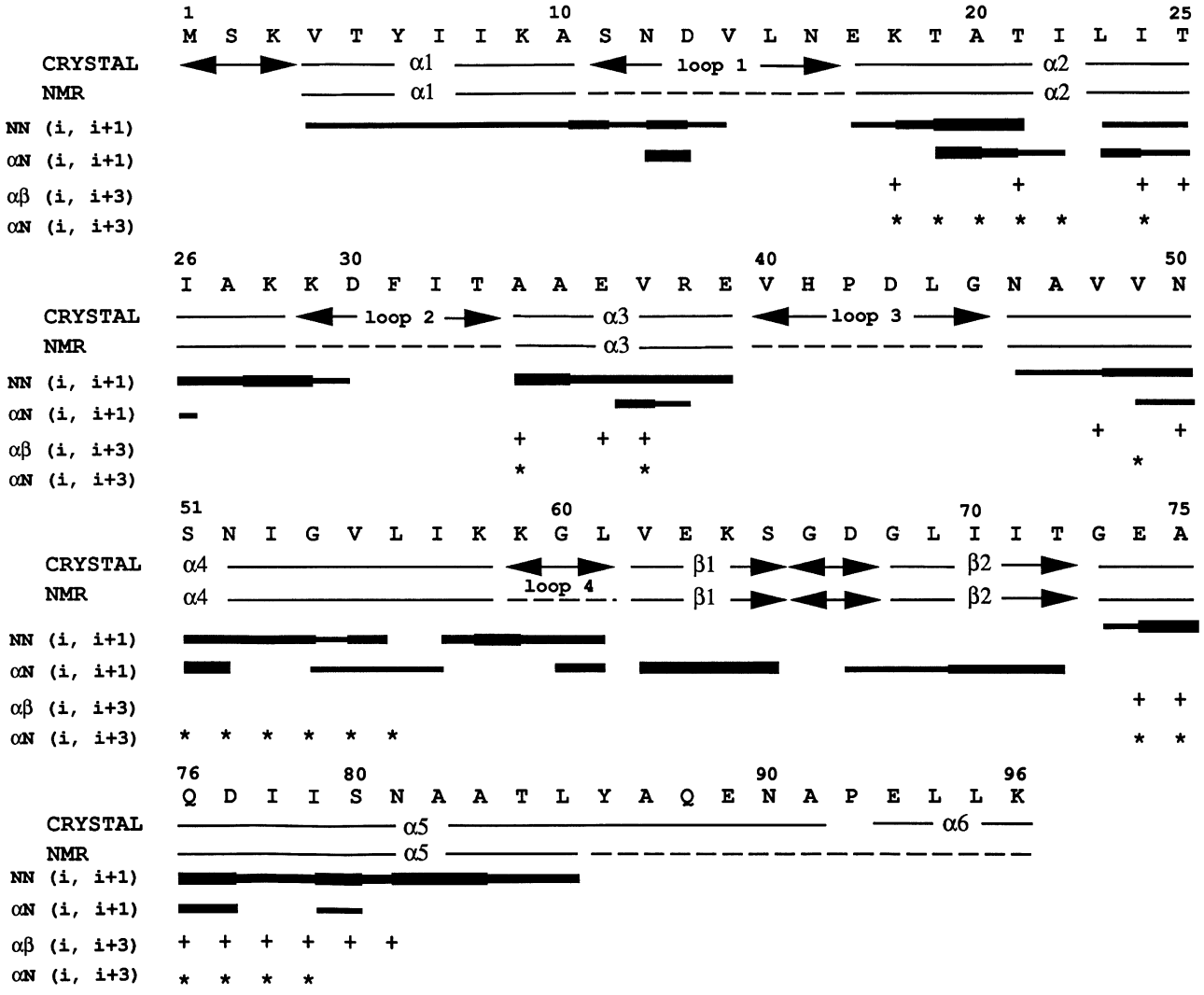

Fig. 1. The primary and secondary structures of MotNF, the N-terminal domain of MotA. The secondary structure of MotNF as determined by NMR and X-ray crystallography superimposed on the amino acid sequence. α-helices are shown as bars, β-strands as arrows and loops as double arrows. The amino acid sequence is shown in the one-letter code. Solid bars indicate consecutive NOE resonances and the bar thickness is proportional to the approximate NOE intensity. An NOE resonance from the α-proton of residue *i* to the β-proton of residue *i* + 3 is shown as a cross. An asterisk indicates an NOE from the α-proton of residue *i* to the amide proton of residue *i* + 3. The dotted lines indicate regions where the inter-residue NOE resonances are not consistent with a defined secondary structure. Note that the three N-terminal residues could not be assigned in the NMR data.

is almost completely α-helical, and it has a distinctive surface patch that contains a mixture of acidic and hydrophobic residues. Mutational studies on the full-length protein argue strongly that this region of MotNF is involved in transcriptional activation. Differences between the X-ray and NMR secondary structures also suggest that MotA forms a dimer when bound to DNA.

Results

NMR studies

Preliminary NMR studies have shown that excellent data can be collected from MotNF in low salt and at low pH (Finnin *et al.*, 1993). This prompted a more extensive NMR analysis to determine the solution structure of the molecule. Initially, the assignment of the NMR peaks was attempted using 2D homonuclear and ^{15}N HMQC spectra. However, as noted previously (Finnin *et al.*, 1993), the spectra have relatively poor dispersion, and more sophisticated three-dimensional experiments were performed using $^{15}N/^{13}C$ doubly-labeled protein to facilitate the analysis. These methods and results are briefly described in this report, and will be presented in greater detail elsewhere.

It was possible to assign the protein backbone from residues 4 to 96, and the side chains were partially assigned using a combination of two-dimensional (2D) and three-dimensional (3D) homonuclear and heteronuclear TOCSY experiments. The side chain assignment was facilitated by the ^{13}C chemical shifts of C_α/C_β pairs which reflect the amino acid type (Grzesiek and Bax, 1993). The entire secondary structure was derived from characteristic patterns of sequential NOE resonances. As suspected from the relatively poor spectral dispersion (Finnin *et al.*, 1993), MotNF is mostly α-helical (Figure 1). The molecule contains five α-helices and a short two-stranded β-ribbon, and residues 1–3 at the N-terminus and 86–96 at the C-terminus appear to be unstructured.

Table I. Statistics for native and derivative data

Crystal	Native1	Native2	SeMet	$KAu(CN)_2$	$HgBr_2$
Concentration (mM)				0.25	1.0
Soaking time (h)				24	24
Resolution (Å)	2.46	2.19	2.5	2.5	2.5
R_{sym} (%)	3.86	5.36	5.32	4.52	8.52
Reflections (measured)	32 150	66 237	33 242	21 227	28 906
Reflections (unique)	7069	9394	5747	6983	6854
Completeness (%)	96.4	98.5	82.0	97.6	97.4

In each case, all data were collected from a single crystal. SeMet is selenomethionine.
$R_{sym} = \Sigma|I_i - I_m|/\Sigma I_m$ where I_i is the intensity of the measured reflection and I_m is the mean intensity of all symmetry-related observations.

Table II. Final phasing data and statistics

Heavy atom	SeMet	$KAu(CN)_2$	$HgBr_2$
Resolution (Å)	2.5	2.5	2.5
Number of sites	2	1	2
Overall phasing power	1.60	1.69	1.53
Mean figure of merit	0.387	0.364	0.411
R_{cullis}	0.608	0.552	0.576

SeMet is selenomethionine. $R_{cullis} = \Sigma|(F_{PH} - F_P) - F_H|/\Sigma|F_{PH} - F_P|$ for centric reflections.
Phasing power = F_H/E_{RMS}; F_P, F_{PH} and F_H are the protein, derivative and heavy atom structure factors respectively, and E_{RMS} is the residual lack of closure.
The overall figure of merit before solvent flattening is 0.517, and the overall figure of merit after solvent flattening is 0.902.

Crystal structure determination

The crystallization of MotNF has been reported previously (Finnin *et al.*, 1993). The crystals are in space group $P3_221$ and contain two molecules in the asymmetric unit. The crystal structure was solved using the multiple isomorphous replacement (MIR) method, and three derivatives were used: selenium, mercury and gold (Tables I and II). The selenium and mercury derivatives required mutagenesis of MotNF since only the gold derivative could be found by conventional crystal soaking methods. Leu85 was replaced with a methionine to permit the metabolic incorporation of selenomethionine, and Asn81 was replaced with a cysteine which was then derivatized with mercury. The molecule was built by several iterative rounds of electron density fitting, phase calculation and phase combination. This process was facilitated by prior determination of the secondary structure using NMR. Equivalent sections of electron density from the initial MIR map and the final $2F_o - F_c$ map are shown in Figure 2. Pertinent statistics for the final refined dimer structure at 2.2 Å are shown in Table III. Note that the mean *B*-factor for molecule B is significantly less than that of molecule A. This is due to the different crystal environments of the two molecules in the asymmetric unit where molecule A is more exposed to the solvent than molecule B.

Description of the structure

The MotNF crystal structure is a dumb-bell shaped dimer of approximate dimensions 60×26×25 Å (Figures 3A and 4). Each monomer is a bundle of five α-helices in which four (α1, α3, α4 and α5) are amphipathic and pack their hydrophobic surfaces around the central helix α2 (Figure 3B). Apart from the C-terminal region (see below), the positions of these α-helices within the primary structure agrees exactly with the NMR results (Figure 1). Also in agreement are the locations of the short β-ribbon and the connecting type II β-turn (Figure 1).

The dimerization is mediated by two interactions involving the α-helical regions at the extreme C-terminus of each monomer. In the first, the C-terminal half of helix α5 projects away from each monomer and interacts with its dimeric partner to form an antiparallel coiled-coil. Alanines 83, 87 and 91 within α5 mediate the short coiled-coil structure (Figure 5A). In the second interaction, the four-residue C-terminal helix α6 from one monomer associates within the body of the other monomer (Figure 5B). This is mediated by a kink between helices α5 and α6 caused by Pro92 which allows Leu94, Leu95 and Tyr86 to associate with their counterparts and create a tight hydrophobic cluster. Lys3, Tyr6, Ile7 and Ile79 also participate in stabilizing interactions with the invading α6 helix. In the NMR secondary structure, helix α5 ends at residue 85 (Figure 1). Therefore, most of the α-helical segments involved in the MotNF dimer crystal structure are apparently absent in solution.

An acidic/hydrophobic surface patch

The GRASP program (Nichols *et al.*, 1991) was used to calculate an accessible surface area and a corresponding surface potential map of the MotNF crystal structure. The surface is relatively smooth with few deep grooves or cavities, but the potential map shows that each monomer is populated with three highly acidic patches. One is on the 'top' of the molecule (relative to Figures 3 and 4) centered on Glu74 and Asp77, the second is 'underneath' the dimer and comprises Glu36, Glu39 and Asp43, and the third is centered on the β-ribbon and includes Asp30, Glu63 and Asp67. An important type of transcriptional activation domain in eukaryotes is the so-called acidic domain which contains neighboring acidic and bulky hydrophobic groups

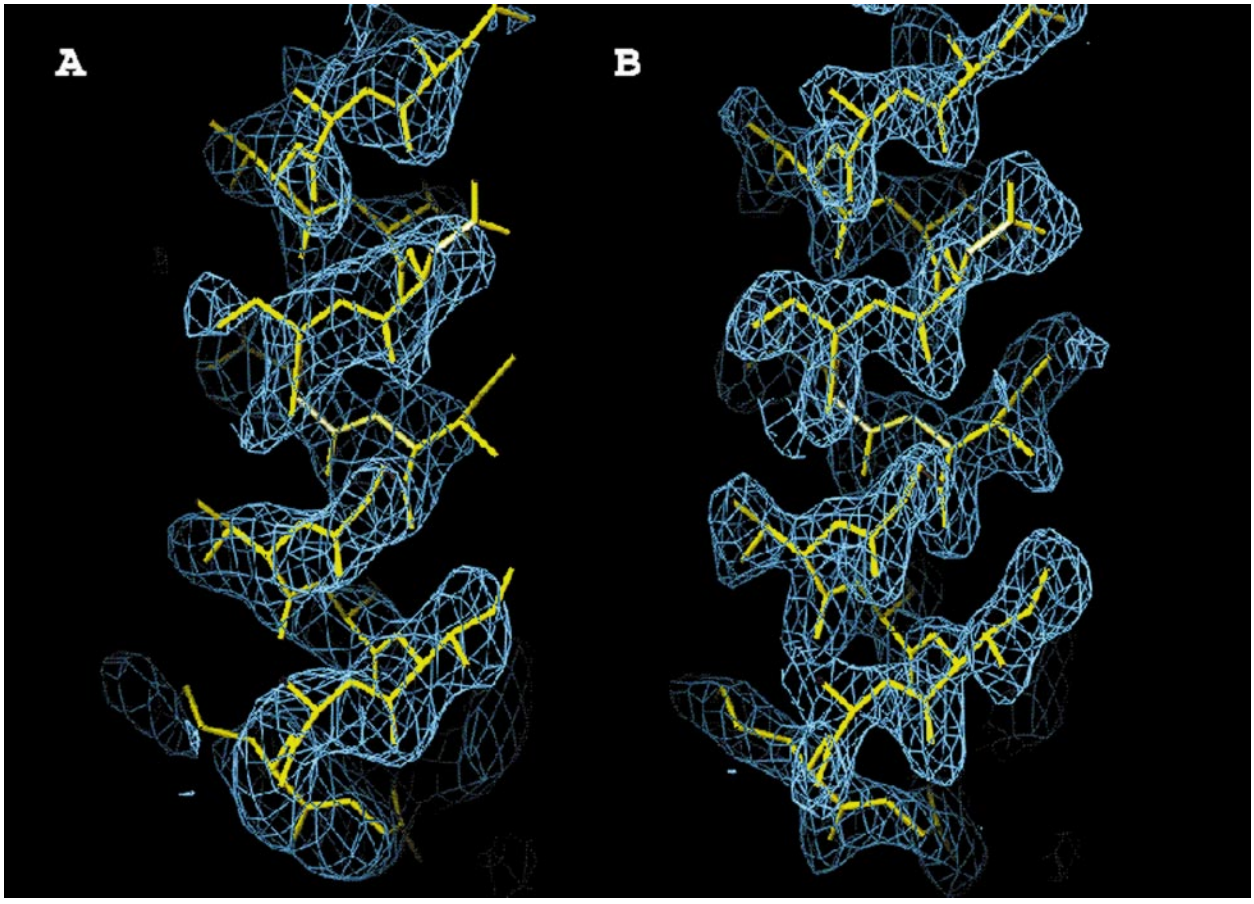

Fig. 2. Electron density maps of MotNF, the N-terminal domain of MotA. Both maps were generated by the O program (Jones *et al.*, 1991) and correspond to the region of the molecule surrounding residues B46–B60 on helix α4. They are contoured at 1.3 σ. (**A**) The initial 2.5 Å MIR map used to build the molecule. (**B**) The final 2.2 Å $2F_o$–F_c map.

which are thought to interact with other elements of the transcription apparatus (Triezenberg, 1995). The third acidic patch on MotNF conforms to this general description since it also contains the adjacent hydrophobic residues Phe31 and Ile70 (Figure 5C and D). The location of this patch on the MotNF dimer is shown in Figure 4.

Mutation of the acidic/hydrophobic patch

A mutational approach was used to assess the importance of this distinctive surface region of MotNF in transcriptional activation. Asp30 and Phe31 were selected for mutagenesis since they are conveniently adjacent within the sequence and are the most prominent elements of the patch. Beginning with a full-length-MotA expression plasmid (Schmidt and Kreuzer, 1992), the two residues were replaced with alanine, in the form of both single (D30A and F31A) and double (D30A/F31A) mutants. The phenotypes caused by these *motA* mutations were analyzed by complementing a *motA* deletion mutant phage from the expression plasmids. The deletion mutant phage does not propagate unless the bacterial host provides MotA protein *in trans* (Benson and Kreuzer, 1992).

Previously isolated *motA* point mutants are viable in normal *E.coli* strains (e.g. strain MCS1) but restricted for growth in a mutant *E.coli* host, TabG. The TabG strain carries a mutation in or near *rpoB* (Pulitzer *et al.*, 1979), which encodes the β-subunit of RNA polymerase. These findings can be rationalized by considering the arrangement of T4 middle-mode genes, which encode several essential replication proteins. The typical T4 middle-mode gene contains a MotA-dependent middle-mode promoter

Table III. Crystallographic parameters of the refined structure

Resolution (Å)	2.2–6.0
Sigma cutoff	2.0
Number of reflections	8781
Completeness of outer shell (2.2–2.29 Å) (%)	97.6
Number of waters	65
Overall *R*-factor	0.208
Overall R_{free}[a]	0.291
Overall *G* factor[b]	0.09
3D–1D profile[c]	0.25–0.65
R.m.s. deviation (α carbons) molecules A and B (Å)[d]	0.971
Mean *B*-factors[d]	
molecule A main chain (Å^2)	32.6
molecule A side chains (Å^2)	35.6
molecule B main chain (Å^2)	24.6
molecule B side chains (Å^2)	29.9
R.m.s. deviation from ideal geometry	
bonds (Å)	0.009
angles (°)	1.71
Ramachandran plot statistics:	
residues in most favored regions (%)	89.4
residues in additional allowed regions (%)	10.6

[a]Brünger (1992).
[b]Laskowski *et al.* (1993).
[c]Luthy *et al.* (1992).
[d]There are two monomers of MotNF in the unit cell.

immediately upstream, and a (MotA-independent) early promoter further upstream (Stitt and Hinton, 1994). The early transcript is thought to require antitermination to extend into the middle gene, and the simplest explanation for restriction by the TabG strain is a defect in this antitermination mechanism. According to this interpretation, MotA activity is required at only a very low level when antitermination is active, but is required at a high level when antitermination of early transcripts is reduced or abolished.

The expression plasmid producing the double-mutant protein allowed the T4 *motA* deletion mutant to form normal-sized plaques in strain MCS1, but did not allow plaque formation in the TabG strain (data not shown). Each single-mutant protein showed a less severe defect, allowing the deletion mutant phage to form small plaques on TabG (and normal plaques on MCS1). The extent of the defects caused by the *motA* mutations was also assessed with a one-step liquid growth experiment in strain TabG. The wild-type expression plasmid permitted a rapid burst of >100 plaque-forming units (p.f.u.) per infected cell, the single D30A mutant plasmid permitted only a delayed and substantially reduced burst, and the single F31A and double D30A/F31A mutants allowed essentially no burst of the *motA* deletion mutant phage even after 90 min of infection (Figure 6). We conclude that both single mutations and the double mutation cause a significant defect in MotA function *in vivo*, with the double D30A/F31A mutation causing the most severe defect. The severity of the double-mutant phenotype is similar to that of previously isolated *motA* point mutants, indicating that the double mutant retains enough activity to allow T4 growth in normal *E.coli* strains.

Structural and functional analysis of D30A/F31A

To analyze the nature of the defect in the D30A/F31A double mutant, the protein was overproduced and purified. We first used NMR to ask whether the mutations grossly affect the structure of the N-terminal domain. MotNF-D30A/F31A was produced from the full-length double-mutant protein by proteolysis (Finnin *et al.*, 1993), and a 2D NOESY spectrum was collected. The spectrum (not

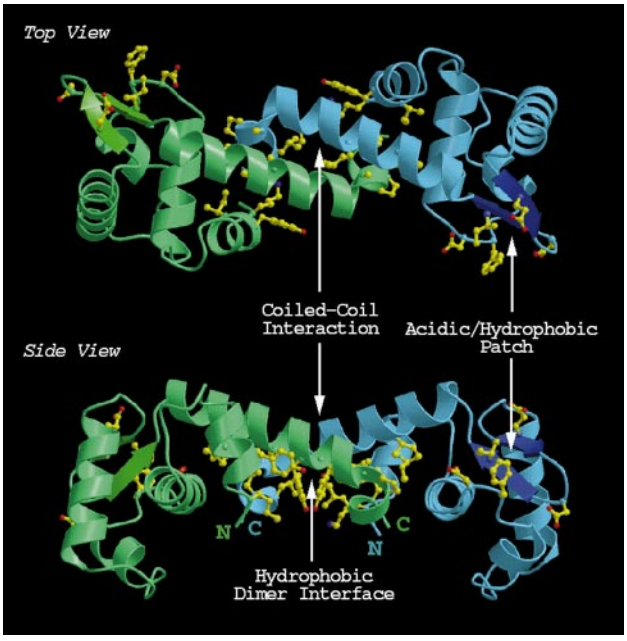

Fig. 4. Important structural and functional features of MotNF: general location. Two orthogonal views of the dimeric crystal structure are shown. Each monomer is coloured separately and the β-ribbons are shaded differently for clarity. The residues involved in the coiled-coil interaction, the hydrophobic dimer interface and the acidic/hydrophobic patch are indicated. These are shown in greater detail in Figure 5. The dimeric structure has two acidic/hydrophobic patches, but only one is labeled. Note the clustering of the N- and C-termini below the dimer close to the hydrophobic interface. The figure was produced with the MOLSCRIPT program (Kraulis, 1991).

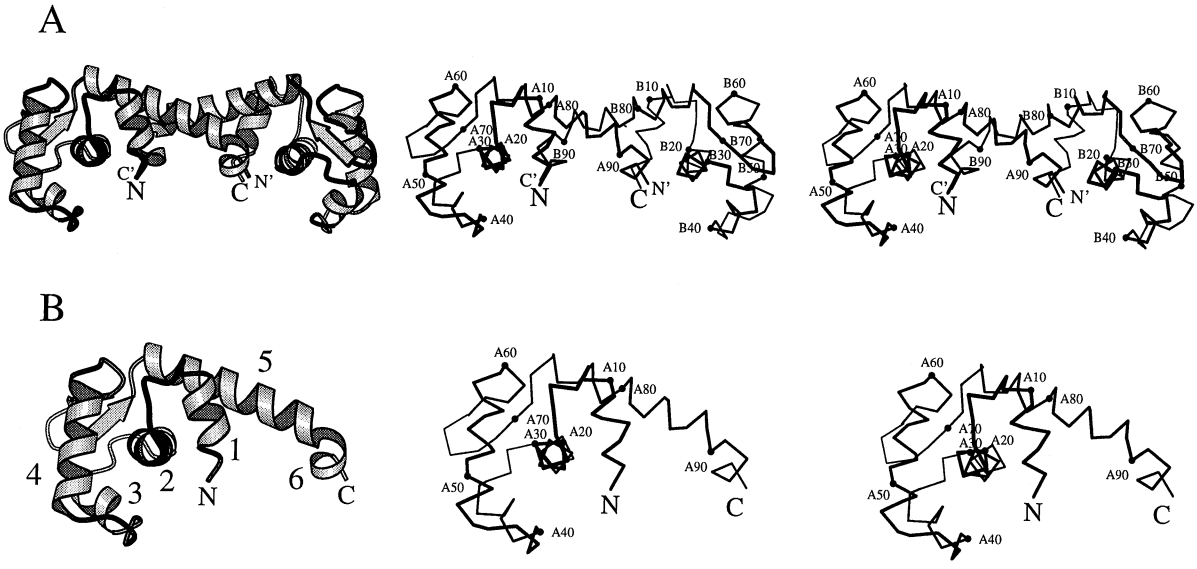

Fig. 3. The 3D structure of MotNF, the N-terminal domain of MotA. (**A**) A ribbon diagram and a stereo diagram of the complete dimer in the crystal asymmetric unit. In the stereo diagram, each α-carbon is shown, and every 10th α-carbon is marked with a dot and numbered. Note that the four termini within the dimer are clustered together at the bottom. (**B**) A ribbon diagram and a stereo diagram of one monomer in the crystal asymmetric unit. The α-helices are numbered in the ribbon diagram from the N- to the C-terminus. The figures were produced with the MOLSCRIPT program (Kraulis, 1991).

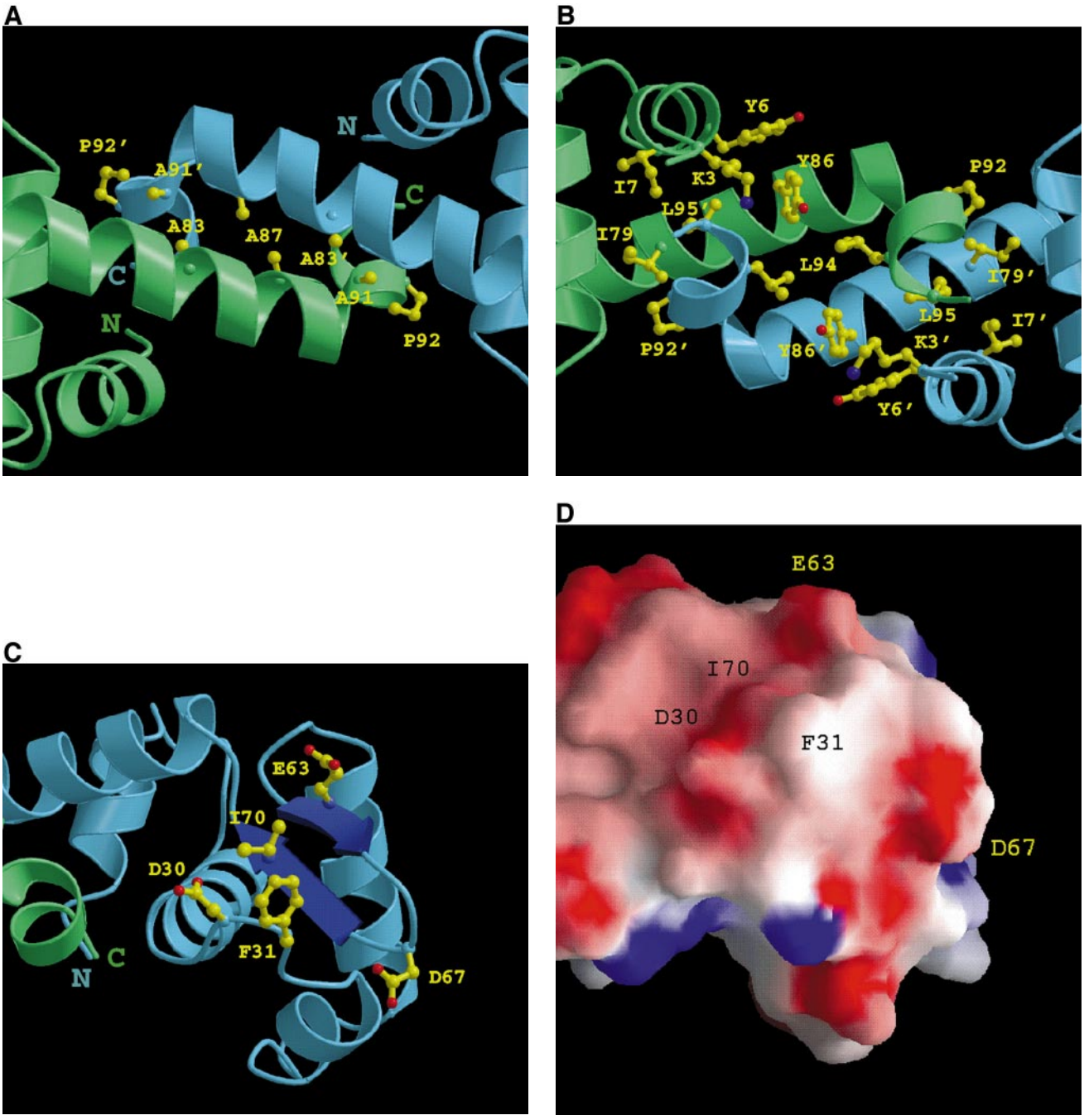

Fig. 5. Important structural and functional features of MotNF: expanded views. (**A**) The alanine residues that mediate the short coiled-coil structure viewed from the 'top' of the molecule. (**B**) The hydrophobic dimer interface viewed from 'below' the molecule. (**C**) The acidic/hydrophobic patch viewed from the 'side' of the molecule. The three figures were produced with the MOLSCRIPT program (Kraulis, 1991). (**D**) The electrostatic surface potential map of the view shown in (C). Red, blue and white correspond to negatively charged, positively charged and uncharged regions respectively. The locations of the important amino acids are shown. The map was generated using the GRASP program (Nichols *et al.*, 1991), and the solvent-accessible surface was calculated with a 1.4 Å probe. The positive upper bound and the negative lower bound for the electrostatic potentials were $+10\ k_bT$ and $-10\ k_bT$, where k_b is the Boltzmann constant and T is the temperature in degrees Kelvin.

shown) confirmed that the overall structure of the double-mutant MotNF protein is very similar to that of wild-type MotNF, consistent with the locations of the two mutated amino acids on the exterior of the molecule. The similar overall structure argues strongly that the *in vivo* phenotype caused by the D30A/F31A mutations is not simply the result of aberrant protein folding.

We next compared site-specific DNA binding by the wild-type and double-mutant MotA proteins, using a gel-shift assay with a 30 bp duplex oligonucleotide containing the –30 region (mot box) of the gene *uvsY* middle-mode promoter. The wild-type protein shifted the oligonucleotide predominantly into a single complex (Figure 7), which reflects site-specific binding to the mot box (Hinton, 1991; Schmidt and Kreuzer, 1992; March-Amegadzie and Hinton, 1995). MotA-D30A/F31A bound the oligonucleotide with essentially the same affinity as the wild-type protein (Figure 7). Therefore, the D30A/F31A mutations do not appear to affect DNA binding, as expected from the prior assignment of the DNA-binding function to

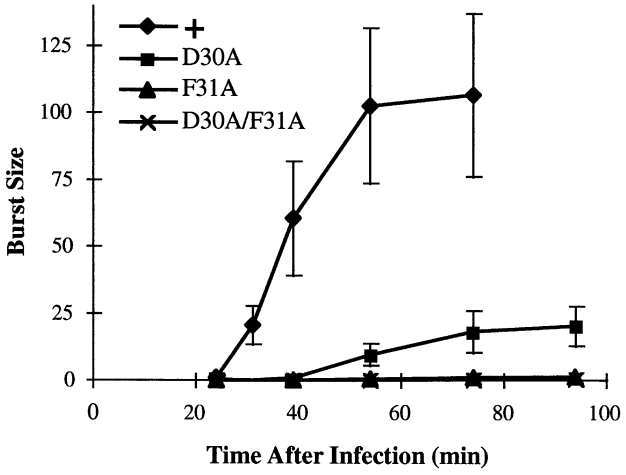

Fig. 6. Burst size analysis with wild-type and mutant MotA. *Escherichia coli* TabG with the indicated MotA expression plasmid was infected with T4 *denA denB motA*Δ and the burst size (per infected cell) was measured as a function of time postinfection by lysing the cells with $CHCl_3$. MotA-F31A and MotA-D30A/F31A did not allow a significant burst throughout the infection.

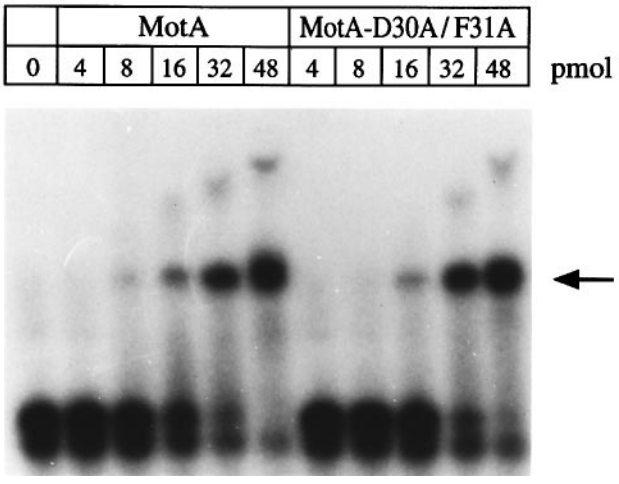

Fig. 7. DNA binding assay with wild-type MotA and MotA-D30A/F31A. An end-labeled 30-mer duplex oligonucleotide containing the mot box from the *uvsY* promoter was incubated with the indicated amount of protein in a 12 μl reaction and subjected to gel electrophoresis under native conditions (see Materials and methods). The primary gel-shift product is indicated by the arrow.

the C-terminal domain of MotA (Finnin *et al.*, 1994; D.M.Hinton, personal communication).

Finally, we analyzed the activation of run-off transcription from the *uvsY* middle-mode promoter by the *E.coli* RNA polymerase in the presence of the co-activator protein AsiA. MotA-D30A/F31A was markedly defective for transcriptional activation (Figure 8A). The mutant protein induced ~11-fold less transcript than the wild-type protein at a low level of MotA (0.1 pmol), and even at saturating MotA levels the amount of transcript was ~4-fold lower with the double-mutant protein (Figure 8B). Based on the defective transcriptional activation but apparently normal DNA-binding activity, we conclude that the D30A/F31A mutant is a positive control mutant of the MotA protein.

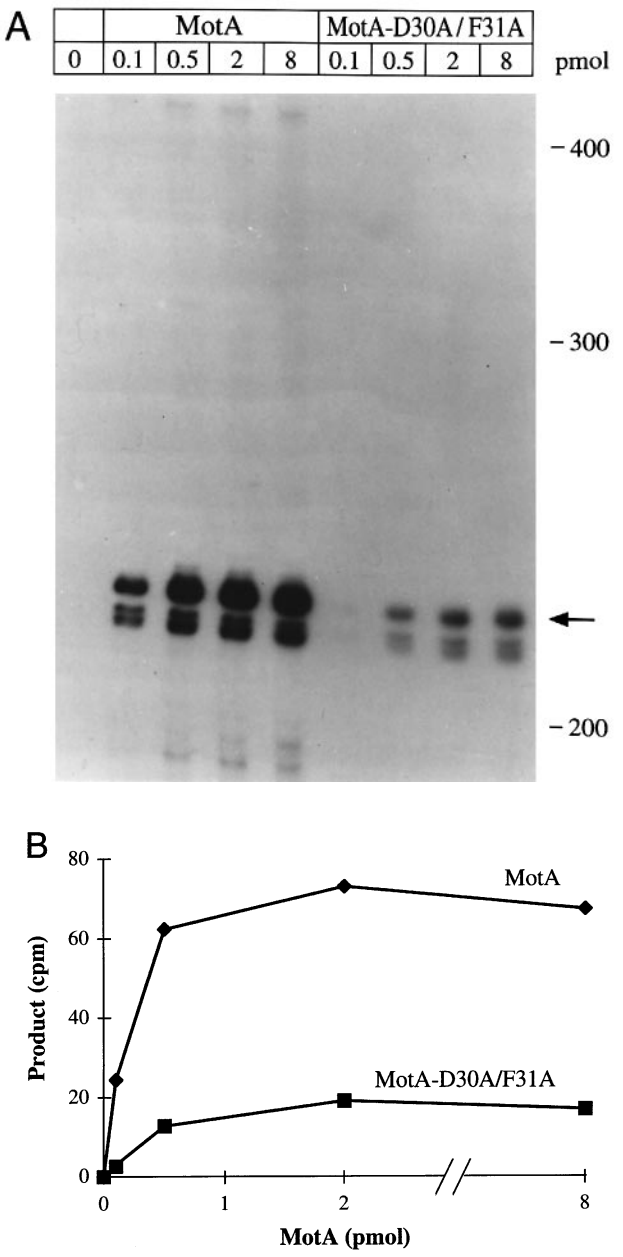

Fig. 8. *In vitro* transcription assay with wild-type MotA and MotA-D30A/F31A. Transcription reactions (21 μl) contained 0.25 pmol *E.coli* RNA polymerase, 7.5 pmol AsiA and the indicated amount of MotA protein (see Materials and methods). (**A**) Autoradiogram of the transcription products run through a polyacrylamide gel. The 221-base transcript (indicated by arrow) was synthesized by run-off transcription using a DNA template containing the *uvsY* middle-mode promoter. Slightly shorter transcripts were probably generated by initiation just downstream from the major initiation site (Ouhammouch *et al.*, 1995); note that the shorter transcripts also require MotA and AsiA proteins. (**B**) Quantitation of transcripts. The major transcript in each lane of the above gel was quantified using an AMBIS direct radioisotope counting system.

Discussion

We have solved the structure of the N-terminal domain of the T4 transcription factor, MotA, and have shown that it contains a conspicuous acidic/hydrophobic patch on its surface. When we mutated two residues of this patch, T4 growth was severely compromised. The double-mutant MotA protein was purified and found to be defective for

transcriptional activation of a middle-mode promoter. The mutations do not disturb the 3D structure of MotA, and the mutant protein appears to bind DNA normally. These results strongly suggest that the surface patch is crucial in mediating protein–protein interactions with T4-modified RNA polymerase during the activation of middle-mode promoters.

The host-encoded RNA polymerase and the T4-encoded AsiA protein are sufficient to elicit MotA-dependent transcriptional activation *in vitro* (Ouhammouch *et al.*, 1995). Therefore, the relevant protein–protein interactions are almost certainly between MotA and one or both of these proteins. Like MotA, AsiA is expressed from an early promoter, and together they induce the transition to middle-mode transcription (for review, see Stitt and Hinton, 1994). AsiA binds to the σ^{70}-subunit of RNA polymerase and probably controls transcription throughout the T4 infection cycle. It participates in the shut-off of transcription from early promoters, causes the RNA polymerase to become MotA dependent for middle promoters, and likely assists late transcription by mediating the replacement of the host σ^{70} by the T4-encoded σ factor, gp55. AsiA and σ^{70} clearly interact closely, but how does MotA interact with the AsiA-containing RNA polymerase?

The σ^{70}-subunit is the most likely target because both proteins contact a similar region of the promoter (centered at –30 for MotA and –35 for σ^{70}). Such an interaction would be reminiscent of that between σ^{70} and the phage λ cI protein, which activates transcription by binding near the –35 region of pRM (see Ptashne, 1992 for review). Recently, a direct interaction has been observed between MotA and σ^{70}, and this interaction was not detected with a mutant of MotA (Mot21) that is defective for transcriptional activation (Gerber and Hinton, 1996). In Mot21, the N-terminal eight residues have been replaced by 11 different residues. Mot21 is the only other positive control mutant of MotA that has been characterized to date. Like the MotA mutants presented in this report, Mot21 retains the DNA-binding properties of the native protein. It is difficult to predict the structural consequences on the MotNF domain caused by the amino acid replacements in Mot21, but the resulting phenotype is consistent with MotNF being the activation domain.

Alternative or additional MotA interactions could include the α-subunit of RNA polymerase and the AsiA protein. Several *E.coli* transcription factors are known to interact with the α-subunit's C-terminal domain. This domain contacts DNA at AT-rich regions upstream of the –35 region and interacts with class I transcription factors, including CRP and OxyR (Ishihama, 1993). If MotA simply interacts directly with the T4-encoded AsiA protein, AsiA might serve as an adaptor between MotA and the host transcription complex.

In addition to the precise interactions that occur between MotA, AsiA and RNA polymerase, a number of key questions remain to be answered about the mechanism of transcriptional activation by MotA and its co-activator protein AsiA. For example, which step(s) in transcriptional initiation is activated (RNA polymerase binding, transition from closed to open complex, etc.)? Does activation also affect later steps in transcription (e.g. promoter clearance)? Is activation at all T4 middle-mode promoters similar, or do unique activation mechanisms come into play? In recent studies with the T4 *uvsX* promoter, March-Amegadzie and Hinton (1995) found that a MotA–RNA polymerase–DNA complex is more stable than a complex of DNA with either protein alone. Furthermore, AsiA-containing RNA polymerase requires MotA in order to form open complexes at the *uvsX* promoter *in vitro* (Hinton *et al.*, 1996). These results suggest that MotA, bound at the mot box in the –30 region, activates an early step involved in open complex formation at the *uvsX* promoter.

Another important question concerns the precise roles of MotA and AsiA in phage DNA synthesis. Replication is severely depressed in both *motA* and *asiA* mutants, and the defect presumably has two causes. First, most of the replication proteins are expressed, at least in part, from middle-mode promoters that require MotA and AsiA for activation. Second, phage replication origins contain middle-mode promoters that appear to be involved directly in the mechanism of replication initiation (for review, see Kreuzer and Morrical, 1994). As expected from their companion roles in regulation and replication, mutants deficient in MotA or AsiA have very similar phenotypes (Ouhammouch *et al.*, 1994).

The differences between the secondary structures of MotNF in solution and in the crystal strongly suggest that the domain can exist in both a monomeric and a dimeric state. This can be explained by assuming that MotA forms a dimer only when immobilized on DNA, and that it is the dimeric form of MotNF that has been captured in the crystal structure. The Stokes radius of MotNF has been measured by gel filtration and dynamic light scattering to be ~19 Å (data not shown), which is also consistent with the monomeric state. If correct, the MotA–DNA interaction would be an example of DNA-directed dimerization, which is a feature of several eukaryotic transcription factors, such as the glucocorticoid receptor (Luisi *et al.*, 1991) and the bZIP proteins (Pabo and Sauer, 1992). In DNA-directed dimerization, the protein binds as two monomers to DNA half-sites, and the aligned molecules then dimerize at their interacting interfaces. The dimerization process adds specificity and stability to the protein–DNA complex. An important feature of the process is the creation of specific protein–protein interactions via conformational changes at the dimer interface. In the case of the MotNF dimer, the highly specific interactions depend completely on the C-terminal α-helical segments, which are apparently missing in solution (Figure 5A and B).

We have previously shown by NMR that the C-terminal DNA-binding domain, MotCF, has similarities to one half of the TBP (Nikolov *et al.*, 1992; Finnin *et al.*, 1994). We have also presented structural evidence that MotCF may bind DNA in a similar fashion to TBP (Kim *et al.*, 1993a,b; Finnin *et al.*, 1994). DNA-directed dimerization is particularly attractive in the case of MotA because TBP is an intramolecular dimer, and dimerization of MotCF would be required to generate the complete TBP-like intermolecular dimer. Since the C-termini of the MotNF dimer project from below the molecule, the putative dimer of MotCF would be positioned below the MotNF dimer as viewed in Figures 3A and 4. We have noted previously that the upper surface of the MotCF β-sheet that would

mediate this interaction with MotNF is highly hydrophobic (Finnin *et al.*, 1994).

Our reason for targeting the acidic/hydrophobic patch of MotNF for mutational and functional analysis is that it contains the types of amino acid that are known to be important components of eukaryotic activation domains. Based on amino acid composition, the latter have been classified into subgroups such as acidic, proline- or glutamine rich (Triezenberg, 1995), and they are normally considered to be largely unstructured. The highly ordered MotNF patch appears not to follow this general description, but recent data suggest that this difference is misleading. First, it is becoming increasingly clear that it is the interspersed hydrophobic residues in eukaryotic activation domains that are important for transactivation (Triezenberg, 1995). Second, in the recently reported structure of the complex between a fragment of the p53 activation domain and the MDM2 oncoprotein, the MDM2–p53 interaction is mediated by three bulky and highly ordered hydrophobic residues from the p53 fragment (Kussie *et al.*, 1996). Thus, the p53 activation domain may be disordered in isolation, but it assumes an ordered α-helical conformation in the protein–protein complex.

Interestingly, there are other features of the MotA system that parallel eukaryotic transcriptional activation. First, activation by MotA requires another phage-encoded protein, AsiA, which seems analogous to eukaryotic co-activator proteins (Ouhammouch *et al.*, 1994, 1995; Brody *et al.*, 1995). Second, MotA contains two domains, a C-terminal domain (MotCF) that binds DNA and an N-terminal domain (MotNF) implicated in transcriptional activation (Finnin *et al.*, 1993; 1994; Gerber and Hinton, 1996; this communication). In prokaryotes, transcription factors generally contain both DNA-binding and activation functions within the same protein domain (Busby and Ebright, 1994). Third, the secondary structure of the DNA-binding domain of MotA is not similar to any known prokaryotic DNA-binding protein, but rather resembles that of the TBP (Nikolov *et al.*, 1992; Finnin *et al.*, 1994). Finally, it is worth noting that T4 replication proteins, including DNA polymerase, polymerase accessory proteins and type II DNA topoisomerase, have both amino acid sequence and functional similarities with their eukaryotic counterparts (Kreuzer and Jongeneel, 1983; Spicer *et al.*, 1988; Tsurimoto and Stillman, 1990; Huff and Kreuzer, 1991). Studies of the MotA system may therefore provide important information relevant to eukaryotic transcriptional activation.

Materials and methods

Bacterial and phage strains

The cloning and expression of the MotNF gene has been described previously (Finnin *et al.*, 1993). To produce the selenium-substituted protein, the L85M mutant gene was expressed in strain B834(DE3), which is auxotrophic for methionine. We have fully described this procedure elsewhere (Golden *et al.*, 1993). *Escherichia coli* strain MCS1 (*supD*) is described by Kreuzer *et al.* (1988) and TabG (Pulitzer *et al.*, 1979) was obtained from L.Gold (University of Colorado, Boulder, CO). Strain JC4583 (F^-, *endA1*, *supE44*, *gal44*, *thi-1*, *thyA48*, *thyR27*, *lac61*) was obtained from P.Modrich (Duke University Medical Center), and DE3 prophage and plasmid pLysE were introduced into the strain by K.Carles-Kinch and K.Kreuzer. T4 *denA* (*nd28*) *denB* (*rII*PT8) and T4 *denA* (*nd28*) *denB* (*rII*PT8) *motA*Δ (Benson and Kreuzer, 1992) were used for all *in vivo* growth assays.

Construction of mutants

The mutants L85M and N81C used in the crystallographic analysis were produced by the PCR protocol developed by Nelson and Long (1989). We have fully described this procedure elsewhere (Golden *et al.*, 1993). Mutations in the acidic/hydrophobic patch were generated by oligonucleotide-directed mutagenesis of pRS31, which contains the cloned full-length *motA* gene (Schmidt and Kreuzer, 1992). A degenerate oligonucleotide spanning the first 109 bases of *motA* (containing the *Nde*I–*Pst*I fragment) was synthesized so that point mutations would be introduced at Asp30 (D30A) and/or Phe31 (F31A). The sequence at these codons was changed from 5′-GATTTC-3′ (normal gene) to 5′-G(A/C)T(T/G)(T/C)T-3′ (oligonucleotide), to change either or both codons to an alanine triplet. The complementary strand was synthesized by primer extension, and the resulting duplex was cleaved with *Nde*I and *Pst*I and then ligated to *Nde*I/*Pst*I-cleaved pRS31. The sequences of the entire *Nde*I–*Pst*I segment of the resulting plasmids were verified by dideoxynucleotide sequencing.

Purification of full-length MotA

The full-length MotA proteins were purified using strain JC4583(DE3) containing plasmid pLysE and a MotA expression plasmid. Cells were grown in 1 l of L broth (10 g/l bactotryptone, 5 g/l yeast extract and 10 g/l NaCl) containing ampicillin (40 μg/ml) to an OD_{560} of 0.8, at which point the cells were induced with isopropyl-β-D-thiogalactopyranoside (IPTG) (0.4 mM final concentration). Cells were grown for an additional 3 h and then pelleted and resuspended in 350 mM potassium phosphate pH 7.6, 1 mM β-mercaptoethanol and lysozyme (200 μg/ml). Polyethyleneimine was added to a final concentration of 1% and DNA was pelleted by centrifugation at 12 000 *g* for 10 min. Ammonium sulfate was added to the supernatant to 80% saturation and the precipitate was pelleted by centrifugation at 17 000 *g* for 30 min. The pellet was resuspended in 30 ml of buffer A [50 mM potassium phosphate pH 7.6, 1 mM β-mercaptoethanol, 100 μM phenylmethanesulfonyl fluoride (PMSF)], and dialyzed against the same buffer for 3 h. The protein was then purified sequentially on an S-Sepharose column and a DEAE–Sepharose column, eluting from both columns with a 0–0.5 M NaCl gradient in buffer A. The MotA protein was dialyzed against buffer A after the first column, and the protein was concentrated to 2 mg/ml using Centricon-10 microconcentrators (Amicon) after the second column. The final pool of MotA was stored in MotA sonication buffer (20 mM Tris–HCl pH 7.9, 1 mM EDTA, 10% glycerol, 1 mM β-mercaptoethanol, 1 mM PMSF) (March-Amegadzie and Hinton, 1995) at –80°C.

Purification of the MotNF domain

The purification procedure for the MotNF domain has been described previously (Finnin *et al.*, 1993). No changes in the protocol were necessary for the mutant and labeled proteins. NMR data for MotNF were collected on unlabeled, ^{15}N-labeled and $^{15}N/^{13}C$ doubly labeled proteins. The procedures used to generate the labeled samples have been described elsewhere (Venters *et al.*, 1991; Finnin *et al.*, 1994; Jaishree *et al.*, 1996).

NMR studies

In all cases, the NMR samples contained 4 mM protein in 200 mM potassium phosphate buffer pH 6.5 and the temperature was 28°C. The 2D homonuclear and HMQC experiments were identical to those used for the MotCF NMR analysis (Finnin *et al.*, 1994). The 3D NMR data were acquired on a Varian Unity 600 MHz spectrometer equipped with a gradient triple resonance probe. This enabled gradient-enhanced versions (Bax and Pochapsky, 1992) of the following spectra to be collected in water: CBCA(CO)NH (Grzesiek and Bax, 1992, 1993; Muhandiram and Kay, 1994), HNCA (Kay *et al.*, 1990), HCCH-TOCSY (Kay *et al.*, 1993), ^{15}N-edited HMQC-NOESY (Fesik and Zuiderweg, 1988) and ^{13}C-edited HSQC-NOESY (Majumdar and Zuiderweg, 1993). Sweep widths of 7400.6, 10 000.0 and 2000 were used for the ^1H, ^{13}C and ^{15}N dimensions respectively. The spectra were referenced with respect to sodium 4,4-dimethyl-4-silapentane-1-sulfonate (DDS) for ^1H, 2.9 M $^{15}NH_4Cl$ in 1 M HCl (24.93 p.p.m.) for ^{15}N and 3-(trimethylsilyl)propanesulfonic acid, sodium salt (TSP) for ^{13}C. For the CBCA(CO)NH and HNCA experiments, 32 increments were collected in the carbon and nitrogen dimensions. The 3D HCCH-TOCSY was acquired using 57 increments in the carbon dimension and a spin lock time of 18.8 ms. For the ^{15}N- and ^{13}C-edited 3D NOESY experiments, 32 and 40 increments were collected in the nitrogen and carbon dimensions respectively with mixing times of 100 ms. All spectra were collected at 28°C. The data were processed using a Gaussian function for apodization in all three dimensions on a SPARC station using VNMR

4.0 (Varian Nuclear Magnetic Resonance Instruments, Palo Alto, CA). Linear prediction was used in the carbon and nitrogen dimensions where applicable.

X-ray data collection and processing

MotNF was crystallized as described previously (Finnin *et al.*, 1993). The crystals are in space group $P3_221$ with unit cell dimensions $a = b = 46.7$ Å, $c = 139.6$ Å. Diffraction data were collected using the oscillation method on an RAXIS-II image plate system mounted on a Rigaku RU300 rotating anode X-ray generator operating at 40 kV and 80 mA (Molecular Structure Corporation). Data were processed by either the RAXIS-II software or the HKL package (Otwinowski, 1993). Typical crystal-to-detector distances and exposure times were 110 mm and 20 min/degree, and the oscillation data were collected in two degree ranges. Isomorphous replacement data were collected from three derivatives, selenium, mercury and gold, and Bijvoet pairs were kept separate initially but later merged. Statistics for both native and derivative data are given in Table I.

Crystal structure solution

The crystal structure was solved using the multiple isomorphous replacement method. Only one derivative, gold, was found by conventional crystal soaking techniques: 0.25 mM $KAu(CN)_2$ for 24 h. Two additional derivatives were generated by appropriate mutagenesis of the protein. Leu85 was replaced by a methionine to permit the metabolic incorporation of selenomethionine, and Asn81 was replaced with a cysteine which was then derivatized by soaking the crystals in 1 mM $HgBr_2$. The heavy atom positions were located by Patterson and difference Fourier methods, and confirmed by cross difference Fouriers. The initial phases had an average figure of merit of 0.517 which improved to 0.902 after density modification. The anomalous data did not improve the phases and were not included in the final phasing. Since the crystal contains two molecules in the asymmetric unit, non-crystallographic symmetry (NCS) averaging was performed in an attempt to improve the phases. The NCS axis was located and refined (correlation coefficient of 0.623 at 4 Å) but the averaging did not improve the map. It was subsequently found that the electron density for one monomer is of considerably poorer quality than the other. The final phasing statistics are shown in Table II. Due to the relatively poor quality of the map, the structure was built in stages using the NMR-derived secondary structure as a guide. Following each round of model building into unambiguous regions of the electron density, phases were calculated and combined with the MIR phases. The final model was refined by alternate rounds of simulated annealing using X-PLOR (Brünger *et al.*, 1987), and rebuilding using $2F_o–F_c$, $F_o–F_c$ and simulated-annealing omit electron density maps (Hodel *et al.*, 1992). Since the structure was built by an iterative procedure, it was carefully checked by a Ramachandran analysis, a 3D–1D profile (Luthy *et al.*, 1992) and PROCHECK (Laskowski *et al.*, 1993). All calculations were performed using the PHASES package (Furey and Swaminathan, 1990) and the molecule was built using the O program (Jones *et al.*, 1991). The final structure included residues 2–96 from both monomers and 65 water molecules. The coordinates of MotNF will be deposited with the Brookhaven Protein Data Bank.

Burst size assay

TabG cells containing the indicated MotA expression plasmid were grown in L broth plus ampicillin (40 μg/ml) to an OD_{560} of 0.5. Cells (5 ml) were then infected with T4 *denA denB motA*Δ at a multiplicity of 0.1 p.f.u./cell, and phage were allowed to attach for 6 min at 37°C without shaking. After attachment, the infected cells were diluted 5000-fold in pre-warmed L broth and then incubated with vigorous aeration at 37°C. At the indicated time point, 1 ml of infected culture was removed and added to 4 ml cold L broth containing $CHCl_3$. Samples were incubated on ice for a minimum of 1 h to allow cell lysis and then each sample was titered on *E.coli* MCS1 containing the wild-type MotA expression plasmid (pRS31). Free (unattached) phage and total phage were titered from samples taken immediately after the 6 min attachment step and diluted 5-fold into L broth with (free phage) and without (total phage) $CHCl_3$. The total phage samples, which include infected cells, were plated immediately onto lawns of MCS1 containing pRS31, while the free phage samples were treated the same as the later time point samples. Burst size was calculated as [(phage titer at indicated time point)–(free phage titer)]/[(total phage titer at 6 min)–(free phage titer)].

Gel-shift assay

The indicated amounts of wild-type MotA or MotA-D30A/F31A were incubated in 12 μl of transcription buffer (10 mM Tris–HCl pH 7.9, 10 mM $MgCl_2$, 100 mM KCl, 1 mM DTT and 100 μg/ml BSA) containing 0.1 pmol DNA template and 5 pmol non-competitive DNA for 10 min at 37°C. 4 μl of loading buffer (10% Ficoll-400, 0.15% bromphenol blue) was then added and the samples were subjected to electrophoresis through a non-denaturing 12% polyacrylamide gel (29:1 total acrylamide:bisacrylamide) in TBE buffer (89 mM Tris base, 89 mM boric acid, 2.5 mM Na_2EDTA) at 4°C and 125 V for 3 h. The DNA template consisted of a 30 bp oligonucleotide (one strand end-labeled with ^{32}P) containing the mot box from the –30 region of the *uvsY* middle-mode promoter. The non-competitive DNA consisted of a 50 bp oligonucleotide from the T4 *uvsW* gene, with no significant matches to the mot box sequence.

In vitro transcription assay

Transcription reactions (21 μl) contained the indicated amounts of wild-type MotA or MotA-D30A/F31A, 7.5 pmol AsiA (kindly provided by Deborah Hinton, NIH, Bethesda, MD), 0.25 pmol RNA polymerase holoenzyme (Boehringer Mannheim), 8 U RNasin (Promega), 0.05 pmol DNA template, 125 μM ATP, 125 μM GTP, 125 μM CTP and 4 μM [α-^{32}P]UTP (30 Ci/mmol) in transcription buffer. The DNA template consisted of the *Ssp*I–*Eco*RV fragment of T4-modified plasmid pGJB1 containing the middle-mode promoter from the T4 *uvsY* gene (Menkens and Kreuzer, 1988), isolated and purified as described by Schmidt and Kreuzer (1992). AsiA and RNA polymerase were pre-incubated for 5 min at 37°C, as were MotA, DNA template and rNTPs. After mixing, the reaction proceeded for 30 min at 37°C and was stopped by adding 80 μl stop solution (77 mM Tris–HCl pH 7.9, 10 mM EDTA, 0.4% SDS). RNA was isolated by ethanol precipitation, resuspended in 6 μl of loading buffer [95% (v/v) formamide, 20 mM Na_2EDTA, 0.05% xylene cyanol, 0.05% bromphenol blue], heated to 90°C for 4 min and subjected to electrophoresis through a denaturing 8% polyacrylamide gel. Markers (BioMarkers Low; BioVentures, Inc.) were end-labeled by kinase treatment and denatured by heating. Electrophoretic bands were quantitated on an AMBIS direct radioisotope counting system.

Acknowledgements

We thank Dr Deborah Hinton for supplying AsiA protein, for providing unpublished data and for many invaluable discussions. We are also grateful to Drs David Hoffman and Ronald Venters for assistance with the NMR analyses, Christine Hughes for help in the Stokes radius measurements, and Drs Dirksen Bussiere and Barbara Golden for many helpful suggestions. This work was partially funded by grant GM34622 from the National Institutes of Health (to K.N.K.) and a generous award from the Rippel Foundation. M.S.F. and M.P.C. were supported by NIH training grant T32CA09111.

References

Bax,A. and Pochapsky,S.S. (1992) Optimized recording of heteronuclear multidimensional NMR spectra using pulsed field gradients. *J. Magn. Reson.*, **99**, 638–643.

Benson,K.H. and Kreuzer,K.N. (1992) Role of MotA transcription factor in bacteriophage T4 DNA replication. *J. Mol. Biol.*, **228**, 88–100.

Brody,E., Rabussay,D. and Hall,D.H. (1983) Regulation of transcription of prereplicative genes. In Mathews,C.K., Kutter,E.M., Mosig,G. and Berget,P.B. (eds), *Bacteriophage T4*. American Society for Microbiology, Washington, DC, pp. 174–183.

Brody,E.N., Kassavetis,G.A., Ouhammouch,M., Sanders,G.M., Tinker, R.L. and Geiduschek,E.P. (1995) Old phage, new insights: two recently recognized mechanisms of transcriptional regulation in bacteriophage T4 development. *FEMS Microbiol. Lett.*, **128**, 1–8.

Brünger,A.T. (1992) Free R value: a novel statistical quantity for assessing the accuracy of crystal structures. *Nature*, **355**, 472–475.

Brünger,A.T., Kuriyan,J. and Karplus,M. (1987) Crystallographic R-factor refinement by molecular dynamics. *J. Mol. Biol.*, **203**, 803–816.

Busby,S. and Ebright,R.H. (1994) Promoter structure, promoter recognition and transcriptional activation in prokaryotes. *Cell*, **79**, 743–746.

deFranciscis,V., Favre,R., Uzan,M., Leautey,J. and Brody,E. (1982) *In vitro* system for middle T4 RNA. II. Studies with T4-modified RNA polymerase. *J. Biol. Chem.*, **257**, 4097–4101.

Fesik,S.W. and Zuiderweg,E.R.P. (1988) Heteronuclear three-dimensional NMR spectroscopy. A strategy for the simplification of homonuclear two-dimensional NMR spectra. *J. Magn. Reson.*, **78**, 588–593.

Finnin,M.S., Hoffman,D.W., Kreuzer,K.N., Porter,S.J., Schmidt,R.P. and White,S.W. (1993) Preliminary structural analysis by X-ray diffraction and nuclear magnetic resonance of the MotA protein from bacteriophage T4. *J. Mol. Biol.*, **232**, 301–304.

Finnin,M.S., Hoffman,D.W. and White,S.W. (1994) The DNA-binding domain of the MotA transcription factor from bacteriophage T4 shows structural similarity to the TATA-binding protein. *Proc. Natl Acad. Sci. USA*, **91**, 10972–10976.

Furey,W. and Swaminathan,S. (1990) PHASES. *Am. Crystallogr. Assoc. Annu. Mtg Program. Abstr.*, **18**, 73.

Gerber,J.S. and Hinton,D.M. (1996) An N-terminal mutation in the bacteriophage T4 *motA* gene yields a protein that binds DNA but is defective for activation of transcription. *J. Bacteriol.*, **178**, 6133–6139.

Golden,B.L., Ramakrishnan,V. and White,S.W. (1993) Ribosomal protein L6: Structural evidence of gene duplication from a primitive RNA-binding protein. *EMBO J.*, **12**, 4901–4908.

Grzesiek,S. and Bax,A. (1992) Correlating backbone amide and side chain resonances in larger proteins by multiple relayed triple resonance NMR. *J. Am. Chem. Soc.*, **114**, 6291–6293.

Grzesiek,S. and Bax,A. (1993) Amino acid type determination in the sequential assignment procedure of uniformly $^{13}C/^{15}N$ enriched proteins. *J. Biomol. NMR*, **3**, 185–204.

Guild,N., Gayle,M., Sweeney,R., Hollingsworth,T., Modeer,T. and Gold,L. (1988) Transcriptional activation of bacteriophage T4 middle promoters by the *motA* protein. *J. Mol. Biol.*, **199**, 241–258.

Hinton,D.M. (1991) Transcription from a bacteriophage T4 middle promoter using T4 motA protein and phage-modified RNA polymerase. *J. Biol. Chem.*, **266**, 18034–18044.

Hinton,D.M., March-Amegadzie,R., Gerber,J.S. and Sharma,M. (1996) Characterization of pre-transcription complexes made at a bacteriophage T4 middle promoter: Involvement of the T4 MotA activator and the T4 AsiA protein, a σ^{70} binding protein, in the formation of the open complex. *J. Mol. Biol.*, **256**, 235–248.

Hodel,A., Kim,S.-H. and Brünger,A.T. (1992) Model bias in macromolecular crystal structures. *Acta Crystallogr.*, **A48**, 851–858.

Huff,A.C. and Kreuzer,K.N. (1991) The mechanism of antitumor drug action in a simple bacteriophage model system. In Potmesil,M. and Ross,W. (eds), *DNA Topoisomerases in Cancer*. Oxford University Press, New York, pp. 215–229.

Ishihama,A. (1993) Protein-protein communication within the transcription apparatus. *J. Bacteriol.*, **175**, 2483–2489.

Jaishree,T.N., Ramakrishnan,V. and White,S.W. (1996) Solution structure of prokaryotic ribosomal protein S17 by high-resolution NMR spectroscopy. *Biochemistry*, **35**, 2845–2853.

Jones,T.A., Zou,J.Y., Cowan,S.W. and Kjeldgaard,M. (1991) Improved methods for building protein models in electron density maps and the location of errors in these models. *Acta Crystallogr.*, **A47**, 110–119.

Kay,L.E., Ikura,M., Tschudin,R. and Bax,A. (1990) Three-dimensional triple-resonance NMR spectroscopy of isotopically enriched proteins. *J. Magn. Reson.*, **89**, 496–514.

Kay,L.E., Xu,G.-Y., Singer,A.U., Muhandiram,D.R. and Kay,J.D.F. (1993) A gradient-enhanced HCCH-TOCSY experiment for recording side-chain ^{1}H and ^{13}C correlations in H_2O samples of proteins. *J. Magn. Reson.*, **101**, 333–337.

Kim,J.L., Nikolov,D.B. and Burley,S.K. (1993a) Co-crystal structure of TBP recognizing the minor groove of a TATA element. *Nature*, **365**, 520–527.

Kim,Y., Geiger,J.H., Hahn,S. and Sigler,P.B. (1993b) Crystal structure of a yeast TBP/TATA-box complex. *Nature*, **365**, 512–520.

Kraulis,P.J. (1991) MOLSCRIPT: a program to produce both detailed and schematic plots of protein structures. *J. Appl. Crystallogr.*, **24**, 946–950.

Kreuzer,K.N. and Jongeneel,C.V. (1983) *Escherichia coli* phage T4 topoisomerase. *Methods Enzymol.*, **100**, 144–160.

Kreuzer,K.N. and Morrical,S.W. (1994) Initiation of DNA replication. In Karam,J.D. (ed.), *Molecular Biology of Bacteriophage T4*. ASM Press, Washington, DC, pp. 28–41.

Kreuzer,K.N., Engman,H.W. and Yap,W.Y. (1988) Tertiary initiation of replication in bacteriophage T4: Deletion of the overlapping *uvsY* promoter/replication origin from the phage genome. *J. Biol. Chem.*, **263**, 11348–11357.

Kussie,P.H., Gorina,S., Marechal,V., Elenbaas,B., Moreau,J., Levine,A.J. and Pavletich,N.P. (1996) Structure of the MDM2 oncoprotein bound to the p53 tumor suppressor transactivation domain. *Science*, **274**, 948–953.

Laskowski,R.A., MacArthur,M.W., Moss,D.S. and Thornton,J.M. (1993) PROCHECK: a program to check the stereochemical quality of protein structures. *J. Appl. Crystallogr.*, **26**, 283–291.

Luisi,B.F., Xu,W.X., Otwinowski,Z., Freedman,L.P., Yamamoto,K.R. and Sigler,P.B. (1991) Crystallographic analysis of the interaction of the glucocorticoid receptor with DNA. *Nature*, **352**, 497–505.

Luthy,R., Bowie,J.U. and Eisenberg,D. (1992) Assessment of protein models with three-dimensional profiles. *Nature*, **356**, 83–85.

Majumdar,A. and Zuiderweg,E.R.P. (1993) Improved ^{13}C-resolved HSQC-NOESY spectra in H_2O using pulsed field gradients. *J. Magn. Reson.*, **102**, 242–244.

March-Amegadzie,R. and Hinton,D.M. (1995) The bacteriophage T4 middle promoter P*uvsX*: Analysis of regions important for binding of the T4 transcriptional activator MotA and for the activation of transcription. *Mol. Microbiol.*, **15**, 649–660.

Menkens,A.E. and Kreuzer,K.N. (1988) Deletion analysis of bacteriophage T4 tertiary origins. A promoter sequence is required for a rifampicin-resistant replication origin. *J. Biol. Chem.*, **263**, 11358–11365.

Muhandiram,D.R. and Kay,L.E. (1994) Gradient-enhanced triple-resonance three-dimensional NMR experiments with improved sensitivity. *J. Magn. Reson.*, **B103**, 203–216.

Nelson,R.M. and Long,G.L. (1989) A general method for site-specific mutagenesis using a modification of the *Thermus aquaticus* polymerase chain reaction. *Anal. Biochem.*, **180**, 147–152.

Nichols,A., Sharp,K.A. and Honig,B.H. (1991) Protein folding and association: insights from the interfacial and thermodynamic properties of hydrocarbons. *Proteins*, **11**, 281–296.

Nikolov,D.B., Hu,S.-H., Lin,J., Gasch,A., Hoffmann,A., Horikoshi,M., Chua,N.-H., Roeder,R.G. and Burley,S.K. (1992) Crystal structure of TFIID TATA-box binding protein. *Nature*, **360**, 40–46.

O'Farrell,P.Z. and Gold,L.M. (1973) Transcription and translation of prereplicative bacteriophage T4 genes *in vitro*. *J. Biol. Chem.*, **248**, 5512–5519.

Orsini,G., Ouhammouch,M., Le Caer,J.-P. and Brody,E.N. (1993) The *asiA* gene of bacteriophage T4 codes for the anti-σ^{70} protein. *J. Bacteriol.*, **175**, 85–93.

Otwinowski,Z. (1993) In Sawyer,L., Isaacs,N. and Bailey,S. (eds), *Proceedings of the CCP4 Study Weekend*. SERC Daresbury Laboratory, Warrington, UK, pp. 56–62.

Ouhammouch,M., Orsini,G. and Brody,E.N. (1994) The *asiA* gene product of bacteriophage T4 is required for middle-mode RNA synthesis. *J. Bacteriol.*, **176**, 3956–3965.

Ouhammouch,M., Adelman,K., Harvey,S.R., Orsini,G. and Brody,E.N. (1995) Bacteriophage T4 MotA and AsiA proteins suffice to direct *Escherichia coli* RNA polymerase to initiate transcription at T4 middle promoters. *Proc. Natl Acad. Sci. USA*, **92**, 1451–1455.

Pabo,C.O. and Sauer,R.T. (1992) Transcription factors: structural families and principles of DNA recognition. *Annu. Rev. Biochem.*, **61**, 1053–1095.

Ptashne,M. (1992) *A Genetic Switch: Phage λ and Higher Organisms*. 2nd edn. Cell Press and Blackwell Scientific, Cambridge, MA.

Ptashne,M. and Gann,A.A. (1990) Activators and targets. *Nature*, **346**, 329–331.

Pulitzer,J.F., Coppo,A. and Caruso,M. (1979) Host-virus interactions in the control of T4 prereplicative transcription. II. Interaction between *tabC*(rho) mutants and T4 *mot* mutants. *J. Mol. Biol.*, **135**, 979–997.

Schmidt,R.P. and Kreuzer,K.N. (1992) Purified MotA protein binds the –30 region of a bacteriophage T4 middle promoter and activates transcription *in vitro*. *J. Biol. Chem.*, **267**, 11399–11407.

Smale,S.T. (1994) Core promoter architecture for eukaryotic protein-coding genes. In Conaway,R.C. and Conaway,J.W. (eds), *Transcription Mechanisms and Regulation*. Raven Press, New York, pp. 63–81.

Spicer,E.K., Rush,J., Fung,C., Reha-Krantz,L.J., Karam,J.D. and Konigsberg,W.H. (1988) Primary structure of T4 DNA polymerase: Evolutionary relatedness to eucaryotic and other procaryotic DNA polymerases. *J. Biol. Chem.*, **263**, 7478–7486.

Stitt,B. and Hinton,D. (1994) Regulation of middle-mode transcription. In Karam,J.D. (ed.), *Molecular Biology of Bacteriophage T4*. ASM Press, Washington, DC, pp. 142–160.

Triezenberg,S.J. (1995) Structure and function of transcriptional activation domains. *Curr. Opin. Genet. Dev.*, **5**, 190–196.

Tsurimoto,T. and Stillman,B. (1990) Functions of replication factor C and proliferating-cell nuclear antigen: Functional similarity of DNA polymerase accessory proteins from human cells and bacteriophage T4. *Proc. Natl Acad. Sci. USA*, **87**, 1023–1027.

Uzan,M., Brody,E. and Favre,R. (1990) Nucleotide sequence and control of transcription of the bacteriophage T4 *motA* regulatory gene. *Mol. Microbiol.*, **4**, 1487–1496.

Venters,R.A., Calderone,T.L., Spicer,L.D. and Fierke,C.A. (1991) Uniform ^{13}C isotope labeling of proteins with sodium acetate for NMR studies: Application to human carbonic anhydrase II. *Biochemistry*, **30**, 4491–4494.

Wilkens,K. and Rüger,W. (1994) Transcription from early promoters. In Karam,J.D. (ed.), *Molecular Biology of Bacteriophage T4*. ASM Press, Washington, DC, pp. 132–141.

Williams,K.P., Kassavetis,G.A., Herendeen,D.R. and Geiduschek,E.P. (1994) Regulation of late gene expression. In Karam,J.D. (ed.), *Molecular Biology of Bacteriophage T4*. ASM Press, Washington, DC, pp. 161–175.

Zawel,L. and Reinberg,D. (1995) Common themes in assembly and function of eukaryotic transcription complexes. *Annu. Rev. Biochem.*, **64**, 533–561.

Received on August 20, 1996; revised on December 2, 1996